


Nucleus accumbens neurons dynamically respond to appetitive and aversive associative learning

Catarina Deseyve^{1,2} | Ana Verónica Domingues^{1,2} | Tawan T. A. Carvalho^{1,2} |
 Gisela Armada^{1,2} | Raquel Correia^{1,2} | Natacha Vieitas-Gaspar^{1,2} | Marcelina Wezik^{1,2} |
 Luísa Pinto^{1,2} | Nuno Sousa^{1,2,3} | Bárbara Coimbra^{1,2} | Ana João Rodrigues^{1,2} |
 Carina Soares-Cunha^{1,2} 

¹Life and Health Sciences Research Institute (ICVS), School of Medicine, University of Minho, Braga, Portugal

²ICVS/3B's-PT Government Associate Laboratory, Braga/Guimarães, Portugal

³Clinical Academic Center-Braga (2CA), Braga, Portugal

Correspondence

Carina Soares-Cunha, ICVS/School of Medicine, University of Minho, Campus de Gualtar, Braga 4710-057, Portugal.
 Email: carinacunha@med.uminho.pt

Funding information

Federation of European Biochemical Societies Excellence Award; International Brain Research Organization Early Career Award; International Society for Neurochemistry Career Development Grant; 'la Caixa' Foundation, Grant/Award Number: 100010434 and LCF/PR/HR20/52400020; European Research Council, Grant/Award Number: 101003187; Fundação para a Ciência e a Tecnologia, Grant/Award Number: 2022.01467.PTDC, 2022.02201.PTDC, 2022.12973.BD, CEECIND/03887/2017, CEECIND/03898/2020, CEECINST/00077/2018, PPBI-POCI-01-0145-FEDER-022122, PTDC/MED-NEU/4804/2020, PTDC/SAU-TOX/6802/2020, SFRH/BD/147066/2019 and UIDB/50026/2020

Abstract

To survive, individuals must learn to associate cues in the environment with emotionally relevant outcomes. This association is partially mediated by the nucleus accumbens (NAc), a key brain region of the reward circuit that is mainly composed by GABAergic medium spiny neurons (MSNs), that express either dopamine receptor D1 or D2. Recent studies showed that both populations can drive reward and aversion, however, the activity of these neurons during appetitive and aversive Pavlovian conditioning remains to be determined. Here, we investigated the relevance of D1- and D2-neurons in associative learning, by measuring calcium transients with fiber photometry during appetitive and aversive Pavlovian tasks in mice. Sucrose was used as a positive valence unconditioned stimulus (US) and foot shock was used as a negative valence US. We show that during appetitive Pavlovian conditioning, D1- and D2-neurons exhibit a general increase in activity in response to the conditioned stimuli (CS). Interestingly, D1- and D2-neurons present distinct changes in activity after sucrose consumption that dynamically evolve throughout learning. During the aversive Pavlovian conditioning, D1- and D2-neurons present an increase in the activity in response to the CS and to the US (shock). Our data support a model in which D1- and D2-neurons are concurrently activated during appetitive and aversive conditioning.

KEYWORDS

aversion, D1-neurons, D2-neurons, nucleus accumbens, Pavlovian conditioning, reward

Abbreviations: 2CA, Clinical Academic Center of Braga; AAV, adeno-associated virus; ANOVA, analysis of variance; AP, anteroposterior; AUC, area under the curve; BLA, basolateral amygdala; CS, conditioned stimuli; DGAV, Direção-Geral de Alimentação e Veterinária; DV, dorsoventral; GuPPy, Guided Photometry Analysis in Python; ICVS, Life and Health Sciences Research Institute; ITI, inter-trial interval; KS, Kolmogorov-Smirnov; ML, mediolateral; MSN, GABAergic medium spiny neuron; NAc, nucleus accumbens; PBS, phosphate-buffered saline; PFA, paraformaldehyde; PFC, prefrontal cortex; PSTH, post-stimulus time histogram; RRID, Research Resource Identifier (see scicrunch.org); US, unconditioned stimulus; VP, ventral pallidum; VTA, ventral tegmental area.

Catarina Deseyve, Ana Verónica Domingues and Tawan T. A. Carvalho contributed equally to this work.

This is an open access article under the terms of the [Creative Commons Attribution-NonCommercial-NoDerivs](https://creativecommons.org/licenses/by-nc-nd/4.0/) License, which permits use and distribution in any medium, provided the original work is properly cited, the use is non-commercial and no modifications or adaptations are made.

© 2024 The Authors. *Journal of Neurochemistry* published by John Wiley & Sons Ltd on behalf of International Society for Neurochemistry.

1 | INTRODUCTION

Daily, species learn and adjust their behavior according to their surroundings. Individuals attribute emotional value to otherwise neutral environmental cues if these are associated with a positive/rewarding or negative/aversive event (Cerri et al., 2014; Rescorla, 1994). These associations, in which a neutral stimulus becomes a conditioned stimulus (CS) once it is paired with an unconditioned stimulus (US) that is inherently rewarding (e.g., food, water or sexual stimuli) or aversive (e.g., shock), are called Pavlovian conditioning. The association transforms the neutral cue into a CS that after learning has the ability to drive rewarding and aversive responses and contributes to learning (Day & Carelli, 2007; Pavlov, 2010).

Lesion and pharmacological evidence indicates that the nucleus accumbens (NAc) is critical for Pavlovian associative learning (Dalley et al., 2005; Di Ciano et al., 2001; Parkinson et al., 2002; Roitman et al., 2005; Setlow et al., 2003). In addition, seminal electrophysiological studies have shown that intraoral administration of sucrose leads to mainly inhibitory responses in NAc neurons, whereas administration of the aversive compound quinine resulted in mainly excitatory responses (Roitman et al., 2005). Interestingly, as associations between CS and US occur, NAc neurons rapidly develop robust responses to the predicting cues (Roitman et al., 2005). Furthermore, it has been shown that NAc neurons increase activity during cue presentations but decrease during reward delivery (Ambroggi et al., 2011; Day et al., 2011; Gale et al., 2014). Similarly, in a Pavlovian conditioning approach task, the majority of recorded accumbal neurons exhibited a significant increase in firing rate during CS presentation, whereas the responses to reward were predominantly inhibitory (Day & Carelli, 2007; Wan & Peoples, 2006).

The NAc is mainly composed of GABAergic medium spiny neurons (MSNs), which account for ~95% of the accumbal neurons, being divided into those that express dopamine receptor D1, dynorphin and substance P (D1-MSNs) or those expressing dopamine receptor D2, enkephalin and adenosine 2a receptor (A2A) (D2-MSNs) (Gerfen, 1984; Gerfen et al., 1990; Le Moine et al., 1991). These two populations also show anatomical segregation, with a significant proportion of D1-MSNs projecting directly to the ventral tegmental area (VTA), forming the direct pathway, and with both populations projecting to the ventral pallidum (VP), forming the indirect pathway (Baimel et al., 2019; Gerfen, 1984; Kupchik et al., 2015; Soares-Cunha & Heinsbroek, 2023). Different studies have shown that both sub-populations are functionally divergent (Hikida et al., 2010; Kravitz et al., 2012; Lobo et al., 2010). However, more recent studies revealed that optogenetic activation of either D1- or D2-neurons in the NAc supports self-stimulation (Cole et al., 2018), and can trigger positive and negative reinforcement (Namvar et al., 2019; Natsubori et al., 2017; Soares-Cunha et al., 2016, 2018, 2020, 2022).

Because of the similar properties between D1- and D2-MSNs in extracellular electrophysiological recordings, it is still unknown which of these populations respond to appetitive and aversive CSs and USs. The development of genetically encoded calcium indicators opened new opportunities to identify these neurons. In the

ventrolateral striatum, calcium elevations in D1- and D2-MSNs were observed at cue presentation in a motivation lever-pressing task (Natsubori et al., 2017). Plus, in a very recent study, putative NAc D1-MSNs presented multiphasic calcium events during CS presentation and reward delivery, whereas D2-MSNs presented a monophasic event only after reward delivery (Skirzewski et al., 2022).

Although some studies point for a role of NAc neurons in cue-reward learning, how D1- and D2-MSNs respond to positive or negative CS-US associations is far from being understood. Thus, to better understand the functional relevance of accumbal D1- or D2-neurons for the acquisition of CS-US Pavlovian learning, we used fiber photometry to register D1- and D2-neurons' activity during appetitive (sucrose) and aversive (foot shock) Pavlovian conditioning in the same animals. We show that D1- and D2-neurons dynamically respond to both cue and reward in the appetitive Pavlovian task. In the aversive Pavlovian task, both neuronal populations increase activity in response to CS and to shock. These results show that both D1- and D2-neurons change activity during reward and aversion processing.

2 | MATERIALS AND METHODS

2.1 | Animals

Male and female heterozygous D1-cre (line EY262, [Gensat.org](https://www.gensat.org); RRID:MMRRC_030989-UCD; $n=7$: $n_{\text{males}}=4$, $n_{\text{females}}=3$) and A2A-cre (line KG139, [Gensat.org](https://www.gensat.org); RRID:MMRRC_036158-UCD; $n=6$: $n_{\text{males}}=3$, $n_{\text{females}}=3$) transgenic mouse lines (2–3 months of age) were used. A2A-cre line was used as to restrict expression to D2-MSNs because D2R is also expressed in cholinergic interneurons (Gallo, 2019). All animals were maintained under standard laboratory conditions: an artificial 12 h light/dark cycle with lights on from 8 am to 8 pm, with an ambient temperature of $21 \pm 1^\circ\text{C}$ and a relative humidity of 50%–60%. Mice were housed in type 2L home cages (3–4 mice per cage), with food (standard diet 4RF21, Mucedola, Italy) and water ad libitum, unless stated otherwise.

Behavioral experiments were performed during the light period of the light/dark cycle. All animals were kept divided according to sex and mouse strain from postnatal day 21. To avoid anxiety and stress responses, 5–10 min of handling was performed 1 week before behavioral experiments began, for 3 consecutive days. Animals were also habituated to all behavioral apparatuses for 3 consecutive days for 15 min before starting the behavioral tasks. Sample size used in behavioral tests was chosen according to previous studies; the investigator was not blind to the group allocation during behavioral performance.

All procedures involving mice were performed according to the guidelines for the welfare of laboratory mice as described in the European Union Directive 2010/63/EU. All protocols were approved by the Ethics Committee of the Life and Health Sciences Research Institute (ICVS) and by the national authority for animal experimentation, Direção-Geral de Alimentação e Veterinária (DGAV; approval reference #8332, dated of 2021-08-05). Health monitoring was

carried out according to FELASA guidelines and all experimenters and animal facilities are accredited by DGAV.

2.2 | D1- and A2A-cre line: Mating and genotyping

The progeny produced by mating a D1-cre or A2A-cre heterozygous transgenic male mouse with a wild-type C57BL/6J female mouse (RRID:IMSR_JAX:000664) was genotyped at weaning (postnatal day 21) by PCR.

DNA was isolated from tail biopsy using the Citogene DNA isolation kit (Citomed, Lisbon, Portugal). In a single PCR genotyping tube, the primers *Drd1a* F1 (5'-GCTATGGAGATGCTCCTGATGGAA-3') and *CreGS* R1 (5'-CGGCAAACGGACAGAAGCATT-3') were used to amplify the D1-cre transgene (340bp) and the primers *Cre* F (5'-AGCCTGTTTTGCACGTTACCC-3') and *Cre* R (5'-GGTTCCCGCAGAACCTGAA-3') to amplify the A2A-cre transgene (300bp). An internal control gene (*lipocalin 2*, 500bp) was used in the PCR (*LCN_1* [5'-GTCCTTCTCACTTTGACAGAAGTCAGG-3'] and *LCN_2* [5'-CACATCTCATGCTGCTCAGATAGCCAC-3']). Heterozygous mice were discriminated from the wild-type mice by the presence of two amplified DNA products corresponding to the transgene and the internal control gene. Gels were visualized with GEL DOC EZ imager (Bio-Rad, Hercules, CA, USA) and analyzed with the Image Lab 4.1 (RRID:SCR_014210; Bio-Rad, Hercules, CA, USA).

2.3 | Surgery and optical fiber implantation

On the day of surgery, D1-cre and A2A-cre mice (2–4 months old) were deeply anesthetized in an induction chamber with 8% sevoflurane (SevoFlo, Abbott, Chicago, IL, USA; in oxygen at 0.8–1 L/min) until loss of paw withdrawal reflex. Then, mice were transferred to a stereotaxic apparatus with anesthesia being given through a nosecone and maintained at 2%–3% (in oxygen at 0.8–1 L/min), to ensure lack of response to mechanical pinch to the hind paw and tail; their body temperature was maintained at 36–37°C using a closed-loop heating pad. An analgesic (buprenorphine) was administered before the beginning of the surgical procedure (0.05 mg/kg, intraperitoneal; Bupaq, RichterPharma, Austria). Animals were injected with the Cre-inducible adeno-associated virus (AAV) AAV5-hSYN-FLEX-GCAMP6f-WPRE-SV40 (RRID:Addgene_100833; 300 nL, Addgene, Watertown, MA, USA) in the NAc [stereotaxic coordinates from bregma (Paxinos & Franklin, 2001): +1.3 mm anteroposterior (AP), 0.9 mm mediolateral (ML), and –4.5 mm dorsoventral (DV)], using a Nanoject III injector (Drumond Scientific Company, Broomall, PA, USA), at a rate of 1 nL/s. After injection, the micropipette was left in place for 5 min to allow viral diffusion.

After viral delivery, a fiber optic ferrule (400 μm core, 0.50 NA; Doric Lenses, Quebec, Canada) was implanted in the NAc using the injection coordinates (except of DV: –4.4) and was then secured to the skull with dental cement (C&B kit, Sun Medical, Shiga, Japan). At

the end of the surgical procedure, mice were removed from the stereotaxic frame and postoperative care was carried out by administering analgesia (0.05 mg/kg buprenorphine; Bupaq, RichterPharma, Austria) 6 h post-procedure, as well as once every 24 h during 3 successive days. A multivitamin supplement (Duphalyte, Zoetis, Spain; diluted 1:10 in 0.9% saline; 20 μL/g, subcutaneous) and 0.9% NaCl (20 μL/g, subcutaneous) were also administered post-procedure, once a day for a maximum of 3 consecutive days, if mice presented signs of dehydration and weakens in movements.

2.4 | Behavioral experiments

All animals performed the appetitive Pavlovian conditioning first and posteriorly (~2 weeks after) the aversive Pavlovian conditioning, to avoid the negative impact caused by foot shock experiments on the appetitive Pavlovian learning.

2.4.1 | Behavioral apparatuses

Behavioral sessions were performed in a custom-made operant chamber using pyControl software and hardware (RRID:SCR_021612; 17.8 cm length × 19 cm width × 23 cm height) within a sound-attenuating box. In the appetitive Pavlovian conditioning, the chamber was composed by a central magazine, to provide access to 15 μL of sucrose solution (20% wt/vol in water) delivered by a solenoid (for liquid dispenser), a cue-sound (70 dB, 5 kHz), and a house-light (100 mA, 2.8 W) installed on the top and metallic floor. For the aversive Pavlovian conditioning, a different chamber containing a house-light (100 mA, 2.8 W) installed on the top of the chamber and a cue-sound (80 dB 2 kHz) and a cue-light installed in one side wall and a gridded floor with shocker was used. A computer was used to control the equipment and record the data, and a webcam (CMOS OV2710, ELP, Shenzhen, China) was used to acquire video.

2.4.2 | Appetitive Pavlovian conditioning (protocol adapted from Patriarchi et al., 2018)

After 3 days of habituation to the behavioral box and the patch cable, mice [$n_{D1-cre} = 7$, $n_{A2A-cre} = 6$; effect size = 0.5 (calculated based on previously published data using a similar behavioral protocol, Patriarchi et al., 2018), power = 0.99] were exposed to 1–2 sessions of sucrose consumption, in which 15 μL of a 20% sucrose solution were delivered every 30 s, for 30 min; this was done for animals to learn the position of the food port. After sucrose consumption session, mice started the appetitive Pavlovian conditioning in which a CS consisting of a 70-dB 5 kHz tone and a house light (100 mA, 2.8 W) were turned on for 10 s; US of 15 μL of 20% sucrose solution was made available at the seventh second after CS onset. CS–US pairings were repeated 30 times per session, with

a variable inter-trial interval (ITI) of 20–35 s (arbitrarily assigned). Mice underwent a total of 12 sessions of appetitive Pavlovian conditioning. The behavior apparatus and the sucrose receptacle were disinfected with 10% ethanol between animals to remove any odor. For all sessions, nose poke data was obtained. Photometry recordings were simultaneously obtained on days 1, 2, and every other day going forward (days 4, 6, 8, 10, and 12), and synchronized through pyControl system and Doric Studio Software (Doric Lenses, Quebec, Canada). The nose pokes performed during each behavioral session were automatically detected through an infrared beam located at the entry of the sucrose port, and licks were detected through a lick detection circuit. Behavioral sessions were also video recorded using a webcam with an infrared light ring (CMOS OV2710, ELP, Shenzhen, China) for posterior analysis of movement.

To quantify CS-triggered behavior, number of nose pokes in the sucrose port during CS were analyzed; nose pokes were also analyzed during the ITI period. Animal movement in the behavioral box was manually scored by an experimenter blind to group allocation on the 12th day of training and was defined as moments of movement initiation (move) and moments of movement pause (rest) when mice were not facing the wall containing the central magazine.

2.4.3 | Aversive Pavlovian conditioning

The same mice [$n_{D1-cre} = 7$, $n_{A2A-cre} = 6$; effect size = 2.83 (calculated based on previously published data using a similar behavioral protocol, de Jong et al., 2019), power = 0.99] were familiarized to the behavior apparatus for 3 days for 10 min with the patch cable connected. Next, mice started a 3-day aversive Pavlovian conditioning protocol. All sessions started with 60 s of habituation period, with the house light on. The CS consisted of an 80-dB, 2 kHz tone plus a cue light. The US was a mild foot shock (0.5 mA, over 1 s). During the first conditioning session, mice were exposed to 10 CS-US pairings. Each trial consisted of a random ITI (45–50 s) followed by a 10-s tone, which was immediately followed by electric foot shock delivered through the stainless steel grid floor. On the second day (US omission), mice performed 30 trials in which 10 out of 30 tones (arbitrarily assigned) were not followed by an electric foot shock. On the third day animals received a US extinction session, in which they received 30 trials with only CS exposure, but without US delivery (protocol adapted from de Jong et al., 2019). All sessions were video recorded with webcams and photometry recordings were simultaneously obtained. To assess CS-triggered aversion, we measured freezing during the CS period from all sessions. The freezing response was manually scored through video observation by an experimenter blind to group allocation and was scored as the time (seconds) that mice spent immobile (lack of any movement including sniffing except respiration during the CS period) and calculated as percentage of total cue time [(freezing time \times 100)/cue duration]. Animal movement in the

behavioral box was assessed on the conditioning day and was defined as moments of freezing initiation (freeze) and moments of freezing cessation (move) during CS and ITI periods.

2.5 | Fiber photometry recordings

Recording of NAc D1- and D2-neuronal activity was performed during appetitive and aversive Pavlovian conditioning, using a Doric Lenses acquisition system (Doric Studio, Quebec, Canada). A fiber optic patch cable (1-m long; 400 μ m core; 0.50NA; Doric Lenses, Quebec, Canada) was coupled to the implanted optic fiber with ceramic sleeve. The system used two LEDs (CLED_465; CLED_405; Doric Lenses, Quebec, Canada) via an LED driver. Excitation light with two different wavelengths of 465 nm for GCaMP6f and 405 nm for the GCaMP6f isosbestic channel, and an emission light were passed through a minicube [iIFMC6-G2_IE(400–410)_E1(460–490)_F1(500–540)_E2(550–580)_F2(600–680)_S; Doric Lenses, Quebec, Canada]. GCaMP signal and a movement control signal from the isosbestic channel were recorded using Doric Studio Software through a console. Light emitted by the indicators is transmitted back through the same optic fiber, split from the illumination light and fluorescence from other indicators by optical filters and converted to electrical signals by one high sensitivity photoreceiver (Newport 2151 with lensed FC adapter; Doric Lenses, Quebec, Canada). The digital inputs are read at the same sampling rate as the analog signals to enable post hoc synchronization of the photometry data with the behavioral hardware. The system uses one digital input to receive a TTL signal each time a behavioral event of interest [reward delivery or foot shock (or foot shock omission)] occurred.

2.6 | Fiber photometry data analysis

Initial analysis was performed in GuPPy (RRID:SCR_022353), Guided Photometry Analysis in Python, a free and open-source package (Sherathiya et al., 2021). The first step was to remove artifacts. GuPPy uses a control channel (isosbestic) that includes smaller movement artifacts and photobleaching artifacts that are subtracted from the signal and used to normalize the data to determine changes from baseline fluorescence ($\Delta F/F$). After establishing a control channel, a fitted control channel is used to calculate $\Delta F/F$ by subtracting the fitted control channel from the signal channel and dividing by the fitted control channel.

After, a post-stimulus time histogram (PSTH) for appetitive Pavlovian conditioning was calculated based on a defined window set around each event timestamp: for CS from –5 s to 7 s (CS onset at 0 s); for US consumption from –5 s to 7 s (US consumption onset at 0 s) – US consumption was considered the first poke mice performed after US delivery that was followed by a licking episode (1 licking episode was defined as having at least 2 lick events occurring less than 250 ms apart). For aversive Pavlovian conditioning, a PSTH spanning from –10 s to 21 s (CS onset at 0 s) was established.

After that, Python packages (Python version 3.9.12, Numpy version 1.21.5; RRID:SCR_006903) were used to calculate the z score from the data present on the PSTH, by subtracting the mean value of baseline activity (-10, 0) for each trial of each animal and dividing by the standard deviation of the baseline activity. To determine any change in fluorescence transients during the PSTH window, a bootstrapping confidence interval (bCI) procedure was used with 95% CI, which was then expanded by a factor of $\sqrt{[n/(n-1)]}$ to account for narrowness bias (Bland & Altman, 2015; Jean-Richard-dit-Bressel et al., 2020). A new z score was generated by randomly re-sampling from trial z score with replacement for the same number of samples. So, n for all statistical analyses of photometry data were the number of trials in each group. This process was repeated 1000 times to create a non-parametric distribution of population mean estimates for each time point within the window. Only periods that were continuously significant (greater or less than the expanded CI limits) for at least 0.5 s were identified as significant (Bland & Altman, 2015; Jean-Richard-dit-Bressel et al., 2020).

The PSTH's mean fluorescence activity (average of the z-score), mean activity, and area under the curve (AUC; using Python package Scikit-learn version 1.1.1 [sklearn.metrics.auc]) in specific periods of time were then calculated. The intervals used for appetitive Pavlovian conditioning data were (time 0s set at CS onset): pre-CS period (-2, 0); post-CS period: (0, 2); pre-US consumption (5, 7); post-US consumption (7, 9). For aversive Pavlovian conditioning data, the intervals were (time 0s set at CS onset): pre-CS period (-2, 0); post-CS period: (0, 2); pre-US period (8, 10); post-US period (10, 12).

The analysis of the GCaMP6f signal ($\Delta F/F$) was conducted using an encoding model (linear regression model) by a multiple-event kernel analysis (Lee et al., 2019; Parker et al., 2016). This signal was modeled as the sum of the responses to each behavioral event, thus determining the contributions of multiple simultaneously modeled events (appetitive Pavlovian conditioning: movement initiation [move], movement cessation [rest], nose poke, CS response, US consumption; aversive Pavlovian conditioning: movement initiation [move], freezing, CS response, US response) to the ongoing GCaMP6f signal. The kernels associated with each event were initially established based on the average signal around 1 s before and 2 s after each individually detected event. By using the least squares method (Python: *scipy.optimize.minimize*, version = 1.8.1, method='Nelder-Mead'), a multiplicative constant for each kernel was optimized so that the sum of the convolutions (from -1 to 2 s) of each kernel with the corresponding behavioral event series best fit the GCaMP6f signal. The behavioral event series are sequences of 0 and 1 s, where 1 s indicates the occurrence of an event. The kernels shown in the figures are the results of the product of the optimized multiplicative constant of each kernel with the initially calculated average signal. The performance of the model for each animal was evaluated using the r -square metric between the average $\Delta F/F$ signal and the model signal across all trials (Python: *sklearn.metrics.r2_score*, version = 1.1.1). The linear regression model successfully captured a significant amount of

variance in the GCaMP6f response (appetitive Pavlovian conditioning: D1 neurons, $r^2 = 0.21 \pm 0.04$, D2 neurons, $r^2 = 0.20 \pm 0.08$; aversive Pavlovian conditioning: D1 neurons, $r^2 = 0.46 \pm 0.02$, D2 neurons, $r^2 = 0.43 \pm 0.03$).

2.7 | Histology

2.7.1 | Euthanasia and brain sectioning

At the end of all behavior procedures, mice were deeply anesthetized by a mixture of ketamine/medetomidine (150 mg/kg/0.3 mg/kg, intraperitoneal). Animals were then transcardially perfused with 0.9% saline, followed by 4% paraformaldehyde (PFA) solution. After, whole heads were immersed for 48 h in 4% PFA so that the fiber track is clearly visible for histological analysis. Next, brains were extracted and then rinsed and stored in 30% sucrose at 4°C until sectioning. Sectioning was performed coronally, in 40 μ m slices, on a vibrating microtome (VT1000S, Leica, Germany) and slices were stored at 4°C on 12-well plates (or long-term storage in cryoprotectant solution at -20°C) until use. Slices from the area of interest (NAc) were selected using the Mouse Brain Atlas (Paxinos & Franklin, 2001).

2.7.2 | Immunostaining (IHC)

To assess GCaMP6f expression in D1-cre and A2A-cre mice, brain slices containing NAc sections with fiber tracks were washed with phosphate-buffered saline (PBS), and then permeabilized with PBS-Triton 0.3% (PBS-T 0.3%). Blocking was performed for 1 h using 5% fetal bovine serum (FBS; cat. no. A5256701, Invitrogen, MA, USA) in PBS-T at RT. The primary antibody goat anti-GFP (1:750; cat. no. ab6673, ABCAM, Cambridge, UK) was incubated overnight at 4°C with agitation, followed by PBS-T washes and subsequent incubation with the secondary fluorescent antibody Alexa Fluor® 488 donkey anti-goat (1:500; cat. no. A11055, Invitrogen, Carlsbad, CA, USA). All antibodies were diluted in PBS-T with 2% FBS. Slices were washed with PBS-T, incubated with 4',6-diamidino-2-phenylindole dihydrochloride (DAPI, 1:1000; cat. no. 62248, Thermo Fisher Scientific™, Waltham, MA, USA) for nucleus staining, washed with PBS, and mounted using Permafluor (cat. no. TA-030-FM, Thermo Fisher Scientific, Hampton, NH, USA). Slides were stored at 4°C and kept protected from light.

2.7.3 | Image acquisition and analysis

Images from the NAc of D1-cre and A2A-cre mice were collected in an inverted confocal microscope (Olympus FV3000, Tokyo, Japan). About 6–8 slices per animal were used for each analysis. Optic fiber placement was assessed to confirm if the activity detected was

from the NAc region. For that, slices where the optic fiber was detected were classified according to the Mouse brain atlas (Paxinos & Franklin, 2001) to estimate the stereotaxic coordinates. All animals contained proper viral expression and fibers were correctly placed in the NAc.

2.8 | Statistical analysis

Statistical analysis was performed in GraphPad Prism 9.0 (RRID:SCR_002798, La Jolla, CA, USA), unless stated otherwise (vide fiber photometry data analysis sub-section). Prior to any statistical comparison between groups, a Tukey's Fences for Outliers test was performed to assess presence of outliers; since no outliers were found, no data points were excluded from the statistical analysis. Normality was assessed in all data analyzed by using the Kolmogorov–Smirnov (KS) test. Parametric tests were used whenever KS test >0.05 . If normality assumptions were not met, non-parametric analysis (Mann–Whitney or Wilcoxon test) was performed.

Initial behavioral analysis comparing male and female mice did not show statistically significant differences (data not shown), thus, males and females were joined in the same groups.

For appetitive Pavlovian conditioning behavior, two-way analysis of variance (ANOVA) for repeated measures was used to assess learning in D1- and A2A-cre mice (factors used: pokes during CS vs. pokes during ITI vs. day of training). Bonferroni's post hoc multiple comparison test was used for group differences determination. Additionally, a linear regression was also performed to assess the correlation between number of nose pokes during CS and days of training.

For the aversive Pavlovian conditioning session (day 1), a one-way ANOVA for repeated measures was applied to analyze percentage (%) of freezing throughout the trials. Statistical analysis between two time points was made using two-tailed paired Student's *t* test to compare percentage of freezing in the first and last trials on day 1 and to compare percentage of freezing in the CS–US trials and CS-only trials on day 2. One-way ANOVA for repeated measures was performed to compare percentage of freezing in the first 5, intermediate 5, and last 5 trials of day 3 of the aversive Pavlovian conditioning.

Regarding fiber photometry data analysis, to assess differences in mean fluorescence before and after CS or US, a two-tailed paired Student's *t* test was used. To determine differences in mean fluorescence from day 1, day 6, and day 12 of appetitive Pavlovian conditioning, a one-way ANOVA for repeated measures was used; Bonferroni's post hoc multiple comparison was used for group differences. To assess differences between AUC of D1- versus D2-neurons, a two-tailed Student's *t* test was used.

Data are presented as mean \pm standard error of the mean (SEM). Individual points are shown in the graphs. Statistical significance was accepted for $p \leq 0.05$. All significant statistical comparisons are presented in the Results section.

3 | RESULTS

3.1 | Mice acquire appetitive Pavlovian conditioning

To examine real-time activity of NAc D1- and D2-neurons in vivo during associative learning, fiber photometry recordings of GCaMP6f fluorescence signals in D1- and A2A-cre mice was conducted (Figure 1a–c; Figure S1a–f). The use of the A2A-cre transgenic mouse line restricts expression to D2-MSNs, excluding the cholinergic interneurons that also express D2R (Gallo, 2019). After multiple sessions of Pavlovian conditioning, both D1- and A2A-cre mice displayed consistent anticipatory poking to the cue, indicating that the cue–reward association had been learned (example of D1-cre mouse in Figure 1d; example of A2A-cre mouse in Figure 1g). D1-cre mice successfully learned the association, given the significantly higher number of pokes/minutes during CS in comparison to ITI (Figure 1e; repeated measures two-way ANOVA; CS vs. ITI: $F_{1,12} = 19.1$, $p = 0.0009$; interaction: $F_{11,132} = 4.0$, $p < 0.001$). Post hoc analysis revealed a significant difference between pokes/minute during CS and ITI starting at day 9 of training (Figure 1e; Bonferroni post hoc; day 9, $p = 0.0123$; day 10, $p = 0.0388$; day 11, $p = 0.0491$; day 12, $p = 0.0094$). In addition, a significant increase in the total number of pokes in the food receptacle during the CS period over days of training was observed (Figure 1f; simple linear regression; $r^2 = 0.2992$, $S = 32.79$, $p < 0.0001$). Similarly, A2A-cre mice successfully learned the association, presenting increased number of pokes during CS in relation to the ITI across days of training (Figure 1h; repeated measures two-way ANOVA; CS vs. ITI: $F_{1,10} = 9.9$, $p = 0.0102$; interaction: $F_{11,110} = 12.39$, $p < 0.0001$). A significant difference between pokes/minute during CS and ITI emerged from day 10 of training forward (Figure 1h; Bonferroni post hoc; day 10, $p = 0.0510$; day 11, $p = 0.0178$; day 12, $p = 0.0060$). A significant increase in total number of total pokes during the CS period across days of training was also observed (Figure 1i; simple linear regression; $r^2 = 0.5739$, $S = 37.37$, $p < 0.0001$).

3.2 | Temporal evolution of NAc D1- and D2-neurons activity during different stages of appetitive conditioning

To verify neuronal activity, we recorded calcium signals from NAc D1- and D2-neurons (using A2A-cre mice) through fiber photometry during appetitive Pavlovian learning.

We divided our analysis in early (day 1), intermediate (day 6), and late (day 12) phases of learning. We used a bootstrapped 95% CI procedure (Bland & Altman, 2015; Jean-Richard-dit-Bressel et al., 2020) to estimate population mean fluorescence (z score) during the 3 s prior and 7 s after each event – CS exposure or US consumption. A significant increase in fluorescence was determined whenever the lower bound of the 95% CI was >0 . Points of statistical significance are represented in the PSTHs colored in red. Given that mice do not consume the reward in all the trials,

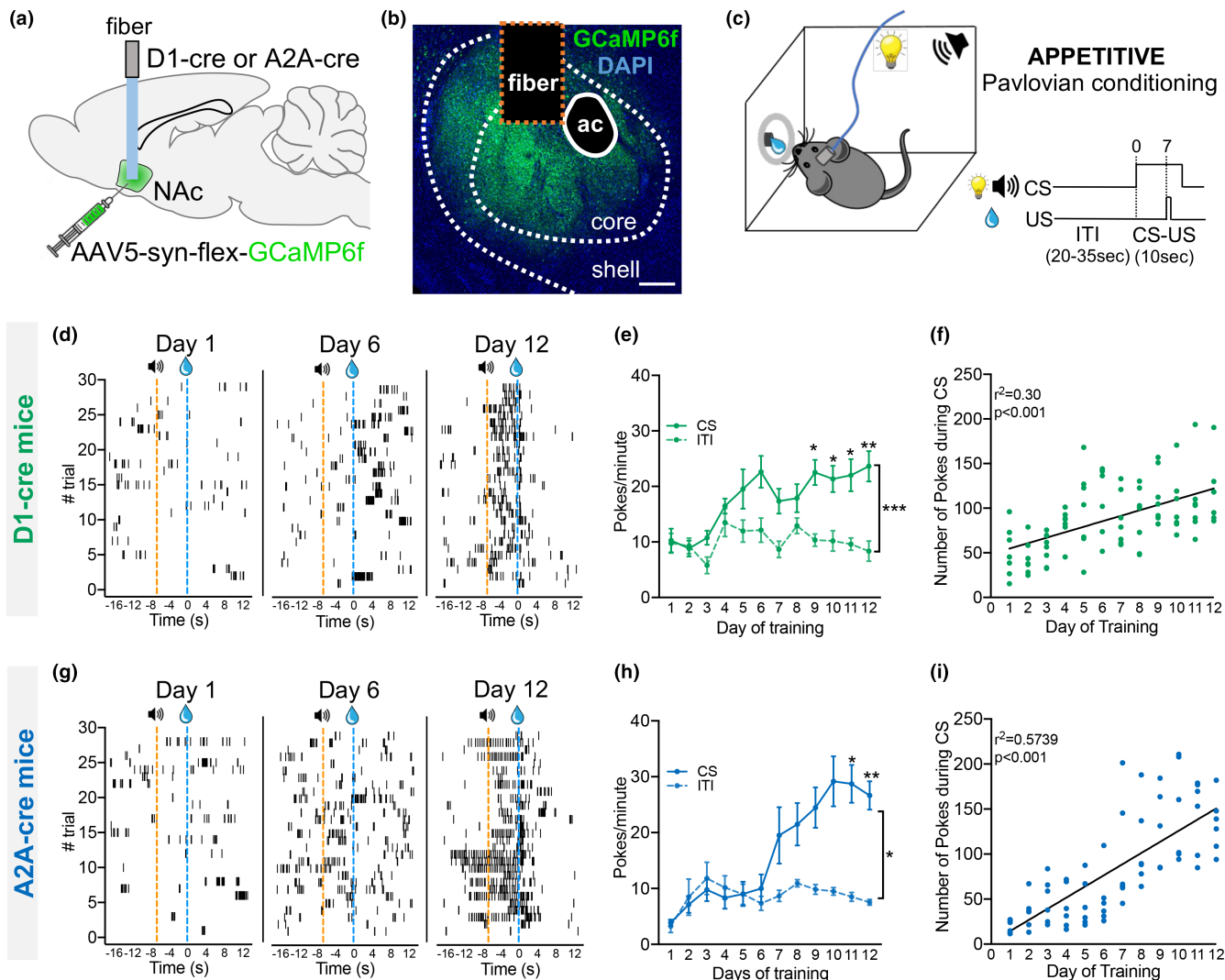


FIGURE 1 Acquisition of appetitive Pavlovian conditioning by D1- and A2A-cre mice during fiber photometry recordings of NAc neurons. (a) Scheme showing the strategy for fiber photometry recording of GCaMP6f in NAc D1- or D2-neurons. (b) Expression of GCaMP6f in the NAc and fiber tip location; scale bar: 250 μm . (c) The appetitive Pavlovian conditioning involved learning to associate a 5-kHz tone and house light (CS) with 20% sucrose reward (US). Representative poke raster of a (d) D1-cre mouse and a (g) A2A-cre mouse, depicting individual pokes that were detected on day 1, day 6, and day 12 of behavioral learning. (e) Number of pokes/minute during CS and ITI in D1-cre mice and in (h) A2A-cre mice. Correlation between number of pokes and Pavlovian session in (f) D1-cre mice and in (i) A2A-cre mice. Data are means \pm SEM. $n_{\text{D1-cre}}=7$ mice; $n_{\text{A2A-cre}}=6$ mice. * $p \leq 0.05$, ** $p \leq 0.01$, *** $p \leq 0.001$. CS, conditioned stimulus; ITI, inter-trial interval; NAc, nucleus accumbens; US, unconditioned stimulus.

especially in the first learning sessions, we only considered for analysis the trials containing both events – CS and US consumption. Nevertheless, the data considering all trials for CS exposure is presented in Figure S2a–k.

Regarding day 1, D1-neurons showed a sharp increase in activity at CS onset, which gradually decreased with time (Figure 2a,d). Analysis of the mean activity 2 s before and 2 s after CS onset shows a significant increase in average activity of D1-cre mice (Figure 2g, left; paired *t* test; $t_5=3.7$, $p=0.0100$). A transient increase in activity after US consumption was observed (Figure 2a,d).

On day 6 of learning, D1-neurons increased activity during CS (Figure 2b,e,h left; paired *t* test; $t_6=3.6$, $p=0.0110$). After reward

consumption, D1-neurons present a sharp decrease in activity (Figure 2b,e,h right; paired *t* test; $t_6=2.3$, $p=0.0500$).

On day 12, we observed a transient increase in fluorescence after CS that returns to baseline some seconds after. After sucrose consumption, D1-neurons decrease activity (Figure 2c,f,i; paired *t* test; CS: $t_5=3.8$, $p=0.0089$), though we observe a posterior increase in activity ~ 3 – 4 s after consumption.

Regarding D2-neurons, on day 1, we observe a slow increase in activity at CS onset, which gradually decreases (Figure 2j,m,p left; paired *t* test; CS: $t_5=3.4$, $p=0.0187$). After reward consumption, D2-neurons activity sharply decreases (Figure 2j,o,p right; paired *t* test; US: $t_5=3.4$, $p=0.0187$).

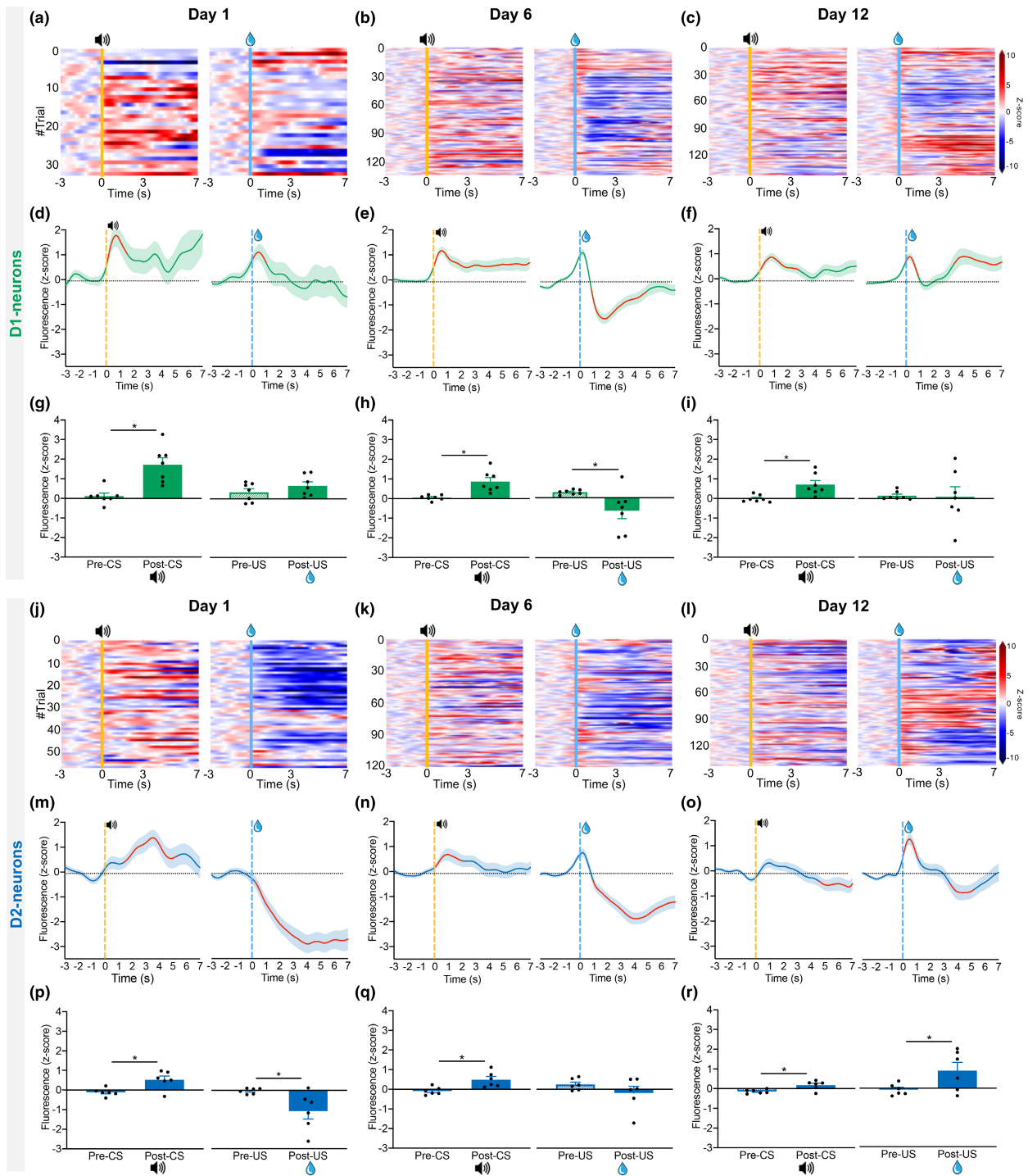


FIGURE 2 Dynamic activity of D1- and D2-neurons during different phases of appetitive Pavlovian conditioning. Heatmaps representing single trial z score activity of D1-neurons in response to CS and US consumption in the first (day 1 – a), intermediate (day 6 – b), and last session (day 12 – c) of appetitive learning. The z-score activity of D1-neurons in response to CS and US consumption in the first (day 1 – d), intermediate (day 6 – e), and last session (day 12 – f) of appetitive learning; red lines on PSTHs represent moments of statistical significance in bootstrapping analysis. Bar graphs showing mean activity of D1-neurons before and after CS or US consumption (day 1 – g; day 6 – h; day 12 – i). Heatmaps representing single trial z-score activity of D2-neurons in response to CS and US consumption in the first (day 1 – j), intermediate (day 6 – k), and last session (day 12 – l) of appetitive learning. The z-score activity of D2-neurons in response to CS and US consumption in the first (day 1 – m), intermediate (day 6 – n), and last session (day 12 – o) of appetitive learning; red lines on PSTHs represent moments of statistical significance in bootstrapping analysis. Bar graphs showing mean activity of D2-neurons before and after CS or US consumption (day 1 – p; day 6 – q; day 12 – r). PSTH data are trial means \pm SEM; bar data are animal means \pm SEM. $n_{D1\text{-cre}} = 7$ mice; $n_{A2A\text{-cre}} = 6$ mice. $**p < 0.01$, $***p < 0.001$.

On day 6, we observed a transient increase in D2-neuronal activity during CS (Figure 2k,n,q left; paired *t* test; CS: $t_5 = 3.1$, $p = 0.0270$), and a decrease in activity after reward consumption (Figure 2k,n right).

On day 12, when learning is fully established, D2-neuronal calcium activity slightly increases at cue onset (Figure 2l,o,r left; paired *t* test; CS: $t_5 = 3.0$, $p = 0.0311$). There is a transient increase in activity in response to US consumption (Figure 2l,o,r right; paired *t* test; US: $t_5 = 2.3$, $p = 0.500$), followed by a decrease afterwards.

As observed in the PSTHs of days 6 and 12, immediately before reward consumption, both neuronal populations present a slight increase in activity. This could reflect motivational or anticipatory signals but could also reflect movement-related activity. Thus, we fitted a linear regression model in which the GCaMP6f signal of D1- or D2-neurons was modeled as the sum of the convolution of different behavioral events with a response kernel that corresponded to that event (Figure S3). The events included signals from movement initiation, rest, pokes, CS and US consumption. To be able to disambiguate between each kernel, we only included signals of events that were not surrounded by other events within a 2-s window. Analysis was focused on the last day of training since this reflects a phase in which CS-US association is consolidated. While we cannot fully exclude the contribution of other events for the observed GCaMP6f signals, the main changes in activity during CS and US consumption are still present when looking at the isolated signals (D1-neurons: Figure S3a-h; D2-neurons: Figure S3i-p). This suggests that cue onset and the consumption of the reward are the main contributors for the activity changes observed after CS and US.

To compare the temporal evolution of the activity of D1- and D2-neurons during learning, we applied a Wilcoxon sum of signed rank analysis to the PSTH for the cue period (0–7 s after CS onset) and US consumption period (0–7 s after US delivery) (Figure S4). Comparison of the fluorescence signals of D1- and D2-neurons during the three phases of learning shows that significant differences exist between neuronal types (Figure S4). On day 1 of training, a significantly higher signal is observed in D1-neurons at CS onset (Figure S4a; Wilcoxon sum of signed ranks, $W = -187394$, $p < 0.0001$) and to the US consumption (Figure S4c; Wilcoxon sum of signed ranks, $W = -417241$, $p < 0.0001$). This difference was further confirmed by a significantly higher AUC in both moments (2 s after event onset; Figure S4b, CS: unpaired *t* test; $t_{11} = 2.2$, $p = 0.0471$; Figure S4d, US: $U_{11} = 4.0$, $p = 0.0140$).

On day 6, D1-neurons' signal was also higher in comparison to D2-neurons in response to CS (Figure S4e,f; Wilcoxon sum of signed ranks, $W = -417241$, $p < 0.0001$). The response to US of the two populations was distinct, with D2-neurons showing lower activity after US onset (Figure S4g,h; Wilcoxon sum of signed ranks, $W = -417241$, $p < 0.0001$).

On day 12, D1- and D2-neurons show distinct magnitude responses during the CS and US (Figure S4i,j, CS: Wilcoxon sum of signed ranks, $W = -417241$, $p < 0.0001$; Figure S4k,l, US: Wilcoxon sum of signed ranks, $W = -270225$, $p < 0.0001$).

These data suggest that both D1- and D2-neurons activity changes throughout learning, and that there are differences between neuronal types.

3.3 | D1- and D2-neuron responses to CS and US activity during appetitive Pavlovian conditioning

Considering the differences between D1- and D2-neurons as learning progresses, we evaluated the average calcium activity in response to CS and US onset over days of the Pavlovian task. To do so, we calculated the average activity of each mouse to CS onset (from 0 to 2 s; considering CS start at 0 s) and to US onset (from 0 to 2 s; considering US consumption at 0 s) across days of training.

Interestingly, the activity of D1-neurons decreases at CS onset over days of training (Figure 3a), with a significant negative correlation between mean activity and days of training (Figure 3a; simple linear regression; $r^2 = 0.09128$, $S = 0.6830$, $p = 0.0349$). The mean fluorescence significantly decreased over days (Figure 3b; repeated measures one-way ANOVA; $F_{3,7} = 4.7$, $p = 0.0394$), though no significant differences between individual days were observed. Regarding US period, no significant correlation between day of training and mean fluorescent was observed (Figure 3c,d).

Regarding D2-neurons, we observed a significant negative correlation between mean activity at CS onset and days of training (simple linear regression; $r^2 = 0.1723$, $S = 0.4370$, $p = 0.0063$; Figure 3e). Mean fluorescence over days was not significantly different. Regarding activity at US consumption, a significant positive correlation between activity at US and days of training was present (simple linear regression; $r^2 = 0.1480$, $S = 1.235$, $p = 0.0119$; Figure 3g). A significant difference across days was found (Figure 3h; repeated measures one-way ANOVA; $F_{3,6} = 1.8$, $p = 0.0288$) with higher fluorescence signals being observed on day 12 in comparison to day 1 (Bonferroni post hoc analysis, day 1 vs. day 12, $p = 0.0003$).

In sum, these results show a gradual decrease in the activity of D1- and D2-neurons in response to CS throughout learning, and a gradual increase in response to US in D2 neurons.

3.4 | Mice acquire freezing responses to aversive Pavlovian conditioning

After the appetitive Pavlovian conditioning, the same mice performed an aversive Pavlovian conditioning paradigm (Figure 4).

On the conditioning session (day 1), we observe an increase in freezing over the trials for both D1-cre (Figure 4b; repeated measures one-way ANOVA; $F_{10,8} = 50.9$, $p < 0.0001$) and A2A-cre mice (Figure 4f; repeated measures one-way ANOVA; $F_{10,6} = 35.58$, $p < 0.0001$). In addition, a significantly higher percentage of freezing was observed in the last trial when compared with the first trial (Figure 4c, paired *t* test; D1-cre: $W_8 = 36$, $p = 0.0078$; Figure 4g, A2A-cre: $t_5 = 16.4$, $p < 0.0001$). In the omission session (day 2), mice still presented a high percentage of freezing responses to the shock-predicting cue (D1-cre: Figure 4d; A2A-cre: Figure 4h). All mice presented similar percentages of freezing in trials with shock delivery or shock omission, which is expected given the random occurrence of omission trials. In the US extinction session (day 3), both D1-cre (Figure 4e) and A2A-cre (Figure 4i) mice presented freezing responses to the shock-predicting cue, despite absence of

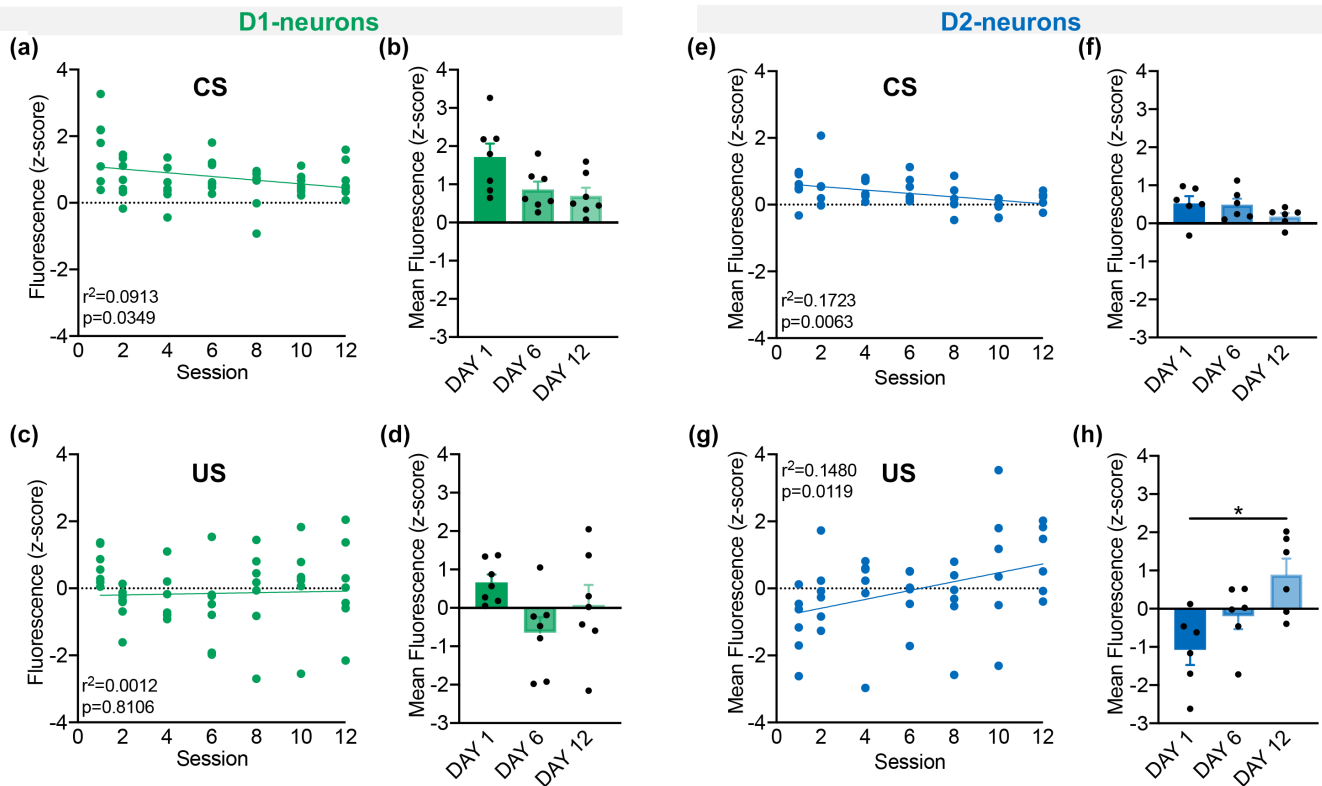


FIGURE 3 Temporal evolution of CS- and US-associated activity of D1- and D2-neurons during appetitive Pavlovian acquisition. Evolution of D1 neuronal activity during (a) CS and (c) US across learning sessions. Quantification of mean fluorescence of D1 neurons in response to (b) CS and (d) US across days of learning (comparison of day 1 vs. day 6 vs. day 12). Evolution of D2 neuronal activity during (e) CS and (g) US across learning sessions. Quantification of mean fluorescence of D2 neurons in response to (f) CS and (h) US across days of learning (comparison of day 1 vs. day 6 vs. day 12). Data are means \pm SEM. $n_{D1\text{-cre}} = 7$ mice; $n_{A2A\text{-cre}} = 6$ mice. * $p \leq 0.05$.

shock, even in the last trials (last 5 out of 30) of the session, indicating presence of CS-triggered fear memory.

3.5 | D1- and D2-neurons activity during aversive Pavlovian conditioning

During all sessions of the aversive Pavlovian conditioning (Figure 4), calcium transients were recorded. Like in appetitive data, we applied a bootstrapped 95% CI procedure to identify activity changes.

On the conditioning day, D1-neurons responded to both CS and US. D1-neurons developed a transient increase in response to the CS (Figure 5a,d,g; $t_6 = 3.4$, $p = 0.0146$). In response to US, D1-neurons developed a robust and sustained increase in activity (Figure 5a,d,g; paired t test; $t_6 = 10.4$, $p < 0.0001$) that started to decrease ~ 3 s after US onset (Figure 5d).

D2-neurons showed a sustained increase in activity in response to the cue (Figure 5j,m,p; paired t test; $t_5 = 4.8$, $p = 0.0048$). In response to the US, D2-neurons showed a sharp significant increase in activity (Figure 5j,m,p; paired t test; $t_5 = 7.3$, $p = 0.0008$), with the activity decreasing to baseline level ~ 2 s after US exposure.

To investigate potential effects of movement or freezing behavior on the activity responses to CS and US, we employed the same regression analysis as described for appetitive behavior. In this case,

we defined four kernels – movement initiation, freezing start, CS, and US (Figure S5). Both populations show responses to CS and US that resemble those from the kernels (D1-neurons: Figure S5a–g; D2-neurons: Figure S5h–n), thus, strongly suggesting that these events are the major contributing factors for the changes in activity observed during the task main events.

Interestingly, comparison of the activity of D1- and D2-neurons during cue (0–10s from CS onset) and US (0–8s from US onset) reveals differences in the temporal evolution of the activity of these populations in the conditioning session (Figure S6). D2-neurons show higher response during the CS period in comparison to D1-neurons (Figure S6a; Wilcoxon sum of signed ranks, $W = 839013$, $p < 0.0001$). Despite the distinct pattern of temporal activity, no differences in AUCs were found (Figure S6b,c).

3.6 | D1- and D2-neurons respond to US omission

On the day after conditioning, mice received 30 trials with 20 CS–US pairings and 10 trials of CS–no US, arbitrarily assigned.

On the CS–US trials, we observed similar activity to what was observed in the conditioning trials on day 1 (Figure 5b,e,h). On the CS–no US trials, D1-neurons increased activity in response to the CS (Figure 5b,e [dashed line],h; paired t test; $t_6 = 2.7$, $p = 0.0500$) until

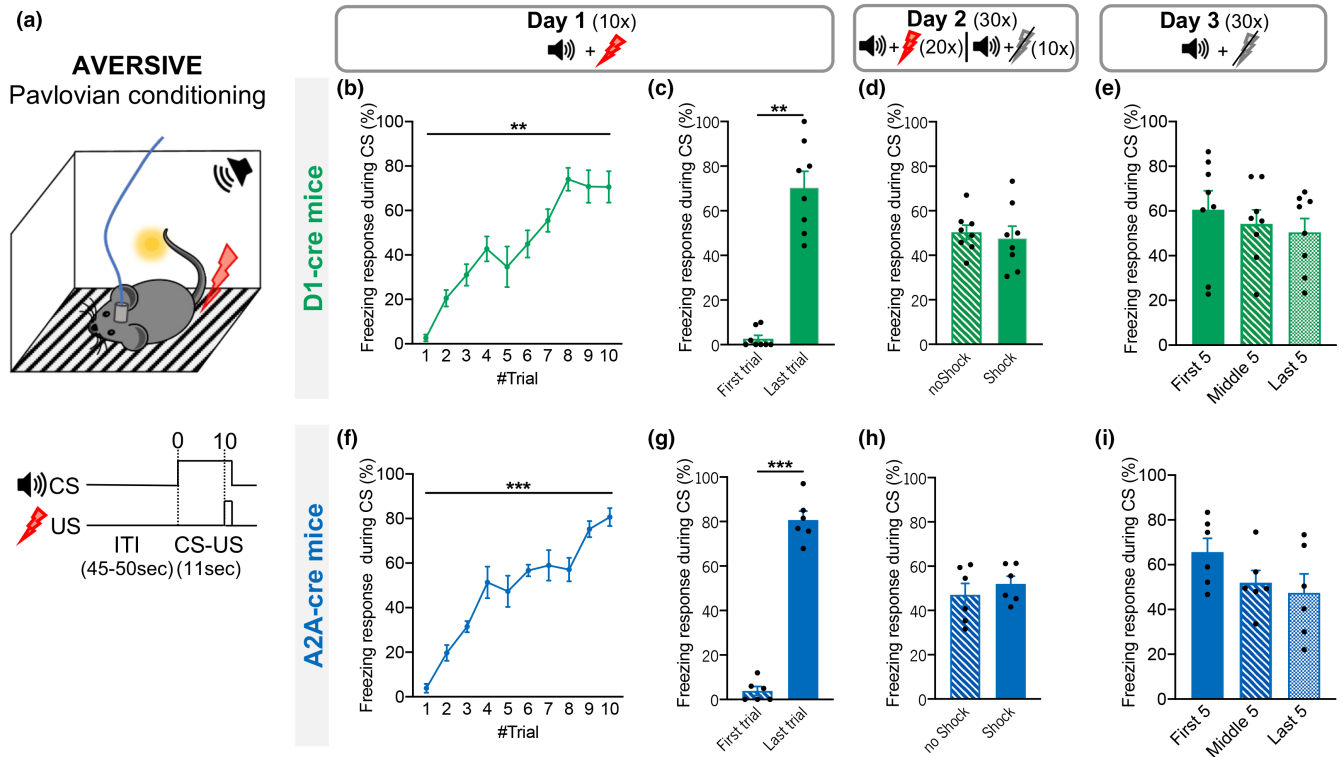


FIGURE 4 Acquisition of aversive Pavlovian conditioning by D1- and D2-cre mice during fiber photometry recordings of NAc neurons. (a) The aversive Pavlovian conditioning involved learning to associate a 2-kHz tone and cue light (CS) with a mild foot shock (US; 0.1 mA, 1 s). Freezing response in the aversive conditioning session of (b) D1-cre and (f) A2A-cre mice. Freezing responses in the last trial were significantly higher than in the first trial in (c) D1-cre mice and (g) A2A-cre mice. In the US omission session (1/3 of trials without US), freezing responses during CS were similar between Shock trials and no-Shock trials for (d) D1-cre mice and (h) A2A-cre mice. In the US extinction trial, both (e) D1-cre mice and (i) A2A-cre mice still present freezing responses to the CS. Data are means \pm SEM. $n_{D1-cre}=7$ mice; $n_{A2A-cre}=6$ mice. $**p \leq 0.01$, $***p \leq 0.001$.

the US, being then followed by a decrease to baseline levels only a few seconds after US omission.

Regarding D2-neurons, on day 2, in the CS-US trials we observe the same as in conditioning day (Figure 5k,n,q). On the CS-no US trials of day 2, D2-neurons presented a sustained increase in activity in response to CS [Figure 5k,n (dashed line), Q; paired *t* test; $t_5=3.1$, $p=0.0272$], until some seconds after US omission.

When analyzing the temporal activity of D1- and D2-neurons, it is possible to observe a more pronounced activation of D2-neurons in comparison to D1-neurons during the CS (Figure S6d; Wilcoxon sum of signed ranks; Shock trials: $W=832363$, $p<0.0001$; no-Shock trials: $W=769527$, $p<0.0001$) and the US (Figure S6d; Wilcoxon sum of signed ranks; Shock trials: $W=541320$, $p<0.0001$; no-Shock trials: $W=438884$, $p<0.0001$). Yet, when looking at AUC of immediate response to either CS or US, no statistically significant differences were found (Figure S6e,f,h,i).

3.7 | D1- and D2-neuron activity in responses to US extinction

On the third day, animals went through an extinction session, in which they were exposed to 30 trials of CS only. Both D1- and D2-neurons' activity increases at CS onset (D1-neurons: Figure 5c,f,i; paired *t* test; $t_5=3.0$, $p=0.0253$ |D2-neurons: Figure 5l,o,r; paired

t test; $t_5=3.3$, $p=0.0226$). In response to shock omission, neither D1-neurons nor D2-neurons significantly change activity, remaining above baseline for some seconds after US omission (D1-neurons: Figure 5c,f,i; D2-neurons: Figure 5l,o,r).

D2-neurons show a significantly higher temporal activity in response to CS in the US omission session, like the conditioning and omission sessions (Figure S6j; Wilcoxon sum of signed ranks, $W=798921$, $p<0.0001$). Yet, AUC of the immediate response to CS (0–2 s from CS onset) was not different between both populations (Figure S6k,l).

In summary, these results show that both D1- and D2-neurons present significant CS responses, with D1-neurons returning to baseline activity before US exposure on the conditioning session and D2-neurons maintaining increased activity over the entire period of CS. In response to the US, a very sharp increase in activity is observed in both populations, though D2-neurons show a faster decay. In the US omission and extinction sessions, both populations show increased activity to the CS, but D2-neurons reveal higher magnitude of response.

4 | DISCUSSION

Accumulating evidence has shown that the NAc plays an important role in mediating Pavlovian associations (Day et al., 2006; Day & Carelli, 2007; Roitman et al., 2005; Wan & Peoples, 2006)

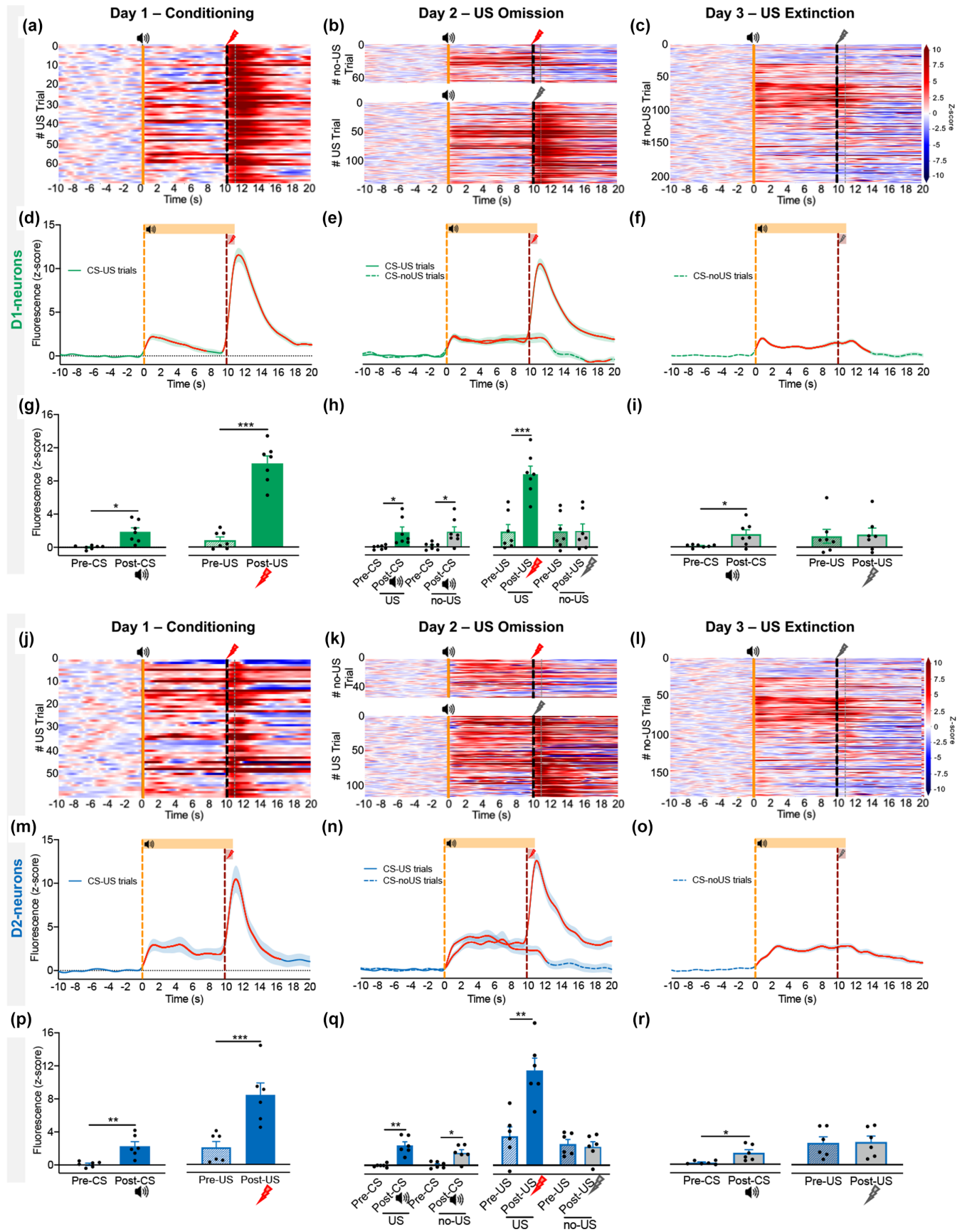


FIGURE 5 Dynamic activity of D1- and D2-neurons during aversive Pavlovian conditioning. Heatmaps representing single trial z-score activity of D1-neurons in the acquisition session (CS–US – a), in the omission session (1/3 of CS–no US trial – b), and in the extinction session (CS–no US – c). The z-score activity of D1-neurons in response to CS and US in the (d) acquisition session, in the (e) omission session, and in the (f) extinction session; red lines on PSTHs represent moments of statistical significance in bootstrapping analysis. Bar graphs showing mean activity of D1-neurons before and after CS or US exposure (acquisition session – g; omission session – h; extinction session – i). Heatmaps representing single trial z-score activity of D2-neurons in the (j) acquisition session, in the (k) omission session, and in the (l) extinction session. The z-score activity of D2-neurons in response to CS and US in the (m) acquisition session, in the (n) omission session, and in the (o) extinction session; red lines on PSTHs represent moments of statistical significance in bootstrapping analysis. Bar graphs showing mean activity of D2-neurons before and after CS or US exposure (acquisition session – p; omission session – q; extinction session – r). PSTH data are trial means \pm SEM; bar data are animal means \pm SEM. $n_{D1-cre} = 7$ mice; $n_{A2A-cre} = 6$ mice. $**p \leq 0.05$, $**p \leq 0.01$, $***p \leq 0.001$.

and that accumbal neurons respond to both CSs and USs (Roitman et al., 2005). However, there is still lack of information about the genetic nature of these neurons. Recent studies from our group have shown that optogenetic manipulation of both D1- and D2-MSNs can trigger positive and negative reinforcement (Soares-Cunha et al., 2020), depending on the pattern of MSN stimulation, suggesting that both populations play a role in positive and negative associative learning. Here, we used fiber photometry to track bulk calcium transients in D1- and D2-neurons during appetitive and aversive Pavlovian conditioning.

Throughout appetitive Pavlovian training, D1- and A2A-cre mice exhibit an increase in the number of nose pokes during CS presentation in relation to ITI, showing that animals learn the association between CS and US (sucrose). Importantly, this behavioral effect was accompanied by a gradual decrease in D1- and D2-neuronal activity during the cue as animals learn the association between CS and US. There is an increase in the activity of D1 and D2 neurons during the CS period in the first day, with a significant decay in the magnitude of this response in subsequent days of training. This suggests that these two NAc sub-populations are dynamically changing activity as Pavlovian associations are acquired. Similarly, seminal electrophysiological studies have shown that NAc neurons develop responses to cues paired with sucrose and quinine (Roitman et al., 2005; Setlow et al., 2003). Although there are studies showing that these sub-populations have an opposing function (Hikida et al., 2010, 2016; Kravitz et al., 2012; Volman et al., 2013), our data show that both populations change activity during appetitive Pavlovian conditioning.

Interestingly, after reward consumption, both D1- and D2-neurons present a decrease in activity, with this effect being more pronounced in D2-neurons. Although the functional role of this asymmetric response needs further investigation, our findings are in accordance with electrophysiological data showing that a large portion of NAc neurons decrease activity during reward delivery (Carelli, 2004; Janak et al., 2004; Roitman et al., 2005). Although we cannot fully exclude the contribution of movement-related changes in activity, the linear regression model revealed that cue onset and the consumption of the reward are the main contributors for the activity changes observed in the calcium data.

We also measured D1- and D2-neurons activity during aversive Pavlovian conditioning in the same animals. As expected, animals exhibit robust freezing behavior in response to the cue in the last

shock trial, in comparison to the first trial of conditioning. Moreover, in trials without shock (days 2 and 3), animals still present freezing responses, showing that the fear association was formed.

Photometry data showed that D1- and D2-neurons also increase activity in response to the CS predicting the aversive US, in line with previous electrophysiological studies of non-identified NAc neurons (Ray et al., 2022; Roitman et al., 2005; Setlow et al., 2003). In the conditioning session, both D1- and D2-neurons present sharp peaks of activity in response to shock. In agreement with our data, electrophysiological recordings in the NAc show that the delivery of quinine, an unpleasant taste US, elicits mainly excitatory responses in NAc neurons (Roitman et al., 2005). In addition, an increase in NAc firing rates was also observed in response to other aversive USs like air puff (Yanagimoto & Maeda, 2003). Importantly, both neuronal populations responded similarly to unexpected omission trials (day 2), as well as to shock extinction conditions (day 3).

Our results corroborate a model of co-existing contribution of D1- and D2-neurons for rewarding and aversive associative learning since both populations show significant activity changes throughout the task and learning. Yet, it is important to refer that fiber photometry calcium imaging reflects bulk population activity, lacking single-cell resolution. Considering recent single-cell RNA sequencing data, at least 18 MSN sub-types exist in the NAc (Chen et al., 2021), suggesting that even within D1- and D2-neurons, functional sub-populations co-exist. Indeed, a study using miniaturized microscopes to monitor single cell activity with calcium indicators in the medial and lateral NAc shell shows distinct types of responses to unexpected rewards (water) in both D1- and D2-MSNs (Chen et al., 2023). This approach or electrophysiological recordings with optogenetic tagging of D1- or D2-neurons would be very interesting to perform in animals during appetitive and aversive Pavlovian conditioning to better understand the contribution of these neurons for these processes. In addition, although recording neuronal activity from the same mouse in both appetitive and aversive learning poses as a great advantage for direct comparison of activity between learning tasks with opposing valence, generalization could occur, possibly impacting on neuronal activity.

Overall, our results show a relevant involvement of both NAc D1- and D2-neurons in reward and aversion processing, in line with previous optogenetic modulation data from our team (Soares-Cunha et al., 2020). Thus, this study reveals that accumbal D1- and D2-neurons present orchestrated and partially overlapping changes

in activity in response to rewarding and aversive events, a process far more complex than the one described by the classical opposing model of ventral basal ganglia function.

AUTHOR CONTRIBUTIONS

Catarina Desevyve: Conceptualization; data curation; formal analysis; investigation; methodology; writing – original draft; writing – review and editing. **Ana Verónica Domingues:** Conceptualization; data curation; formal analysis; investigation; methodology; writing – original draft; writing – review and editing. **Tawan T. A. Carvalho:** Conceptualization; data curation; formal analysis; investigation; writing – review and editing. **Gisela Armada:** Data curation; formal analysis; investigation; writing – review and editing. **Raquel Correia:** Formal analysis; investigation; writing – review and editing. **Natacha Veitas-Gaspar:** Data curation; investigation; writing – review and editing. **Marcelina Wezik:** Formal analysis; investigation; writing – review and editing. **Luísa Pinto:** Investigation; writing – review and editing. **Nuno Sousa:** Investigation; writing – review and editing. **Bárbara Coimbra:** Data curation; formal analysis; investigation; writing – review and editing. **Ana João Rodrigues:** Funding acquisition; investigation; writing – original draft; writing – review and editing. **Carina Soares-Cunha:** Conceptualization; formal analysis; funding acquisition; investigation; project administration; supervision; validation; visualization; writing – original draft; writing – review and editing.

ACKNOWLEDGMENTS

CS-C, BC and LP have Scientific Employment Stimulus contracts from the Portuguese Foundation for Science and Technology (FCT) (CEECIND/03887/2017 [DOI: [10.54499/CEECIND/03887/2017/CP1458/CT0027](https://doi.org/10.54499/CEECIND/03887/2017/CP1458/CT0027)]; CEECIND/03898/2020 [DOI: [10.54499/2020.03898.CEECIND/CP1600/CT0015](https://doi.org/10.54499/2020.03898.CEECIND/CP1600/CT0015)]; CEECINST/00077/2018 [DOI: [10.54499/CEECINST/00077/2018/CP1640/CT0003](https://doi.org/10.54499/CEECINST/00077/2018/CP1640/CT0003)]). AVD and NG have FCT PhD grants (SFRH/BD/147066/2019; 2022.12973.BD).

This work received funding from the Bial Foundation grant (175/2020). In addition, part of the experiments was funded by the European Research Council (ERC) under the European Union's Horizon 2020 research and innovation program (grant agreement no. 101003187) and by the “la Caixa” Foundation (ID 100010434), under the agreement LCF/PR/HR20/52400020. Part of the work received funding from Portuguese Foundation for Science and Technology (FCT) under the scope of the projects PTDC/MED-NEU/4804/2020 (DOI: [10.54499/PTDC/MED-NEU/4804/2020](https://doi.org/10.54499/PTDC/MED-NEU/4804/2020)), PTDC/SAU-TOX/6802/2020 (DOI: [10.54499/PTDC/SAU-TOX/6802/2020](https://doi.org/10.54499/PTDC/SAU-TOX/6802/2020)), 2022.02201.PTDC (DOI: [10.54499/2022.02201.PTDC](https://doi.org/10.54499/2022.02201.PTDC)), and 2022.01467.PTDC (DOI: [10.54499/2022.01467.PTDC](https://doi.org/10.54499/2022.01467.PTDC)).

This work was also supported by a FEBS (Federation of European Biochemical Societies) Excellence Award (2022), IBRO Early Career Award (2022), “Maria de Sousa” Award and ISN (international Society for Neurochemistry) Career Development Grant, attributed to CS-C.

Part of this work received funding from the ICVSS Scientific Microscopy Platform, member of the national infrastructure PPBI – Portuguese Platform of Bioimaging (PPBI-POCI-01-0145-FEDER-02212); and by National funds, through the FCT – UIDB/50026/2020 (DOI: [10.54499/UIDB/50026/2020](https://doi.org/10.54499/UIDB/50026/2020)) and UIDP/50026/2020 (DOI: [10.54499/UIDP/50026/2020](https://doi.org/10.54499/UIDP/50026/2020)).

UIDB/50026/2020) and UIDP/50026/2020 (DOI: [10.54499/UIDP/50026/2020](https://doi.org/10.54499/UIDP/50026/2020)).

CONFLICT OF INTEREST STATEMENT

No conflicts of interests to declare.

PEER REVIEW

The peer review history for this article is available at <https://www.webofscience.com/api/gateway/wos/peer-review/10.1111/jnc.16063>.

DATA AVAILABILITY STATEMENT

The data that support the findings of this study are available from the corresponding author upon reasonable request.

A preprint of this article was posted on April 21, 2023: <https://www.biorxiv.org/content/10.1101/2023.04.21.537763v1.full>.

ORCID

Carina Soares-Cunha  <https://orcid.org/0000-0001-9470-644X>

REFERENCES

- Ambroggi, F., Ghazizadeh, A., Nicola, S. M., & Fields, H. L. (2011). Roles of nucleus accumbens core and shell in incentive-cue responding and behavioral inhibition. *The Journal of Neuroscience*, 31, 6820–6830. <https://doi.org/10.1523/JNEUROSCI.6491-10.2011>
- Baimel, C., McGarry, L. M., & Carter, A. G. (2019). The projection targets of medium spiny neurons govern cocaine-evoked synaptic plasticity in the nucleus accumbens. *Cell Reports*, 28, 2256–2263.e3. <https://doi.org/10.1016/j.celrep.2019.07.074>
- Bland, J. M., & Altman, D. G. (2015). Statistics notes: Bootstrap resampling methods. *BMJ*, 350, h2622. <https://doi.org/10.1136/bmj.h2622>
- Carelli, R. M. (2004). Nucleus accumbens cell firing and rapid dopamine signaling during goal-directed behaviors in rats. *Neuropharmacology*, 47, 180–189. <https://doi.org/10.1016/j.neuropharm.2004.07.017>
- Cerri, D. H., Saddoris, M. P., & Carelli, R. M. (2014). Nucleus accumbens core neurons encode value-independent associations necessary for sensory preconditioning. *Behavioral Neuroscience*, 128, 567–578. <https://doi.org/10.1037/a0037797>
- Chen, G., Lai, S., Bao, G., Ke, J., Meng, X., Lu, S., Wu, X., Xu, H., Wu, F., Xu, Y., Xu, F., Bi, G.-Q., Peng, G., Zhou, K., & Zhu, Y. (2023). Distinct reward processing by subregions of the nucleus accumbens. *Cell Reports*, 42, 112069. <https://doi.org/10.1016/j.celrep.2023.112069>
- Chen, R., Blosser, T. R., Djekidel, M. N., Hao, J., Bhattacharjee, A., Chen, W., Tuesta, L. M., Zhuang, X., & Zhang, Y. (2021). Decoding molecular and cellular heterogeneity of mouse nucleus accumbens. *Nature Neuroscience*, 24, 1757–1771. <https://doi.org/10.1038/s41593-021-00938-x>
- Cole, S. L., Robinson, M. J. F., & Berridge, K. C. (2018). Optogenetic self-stimulation in the nucleus accumbens: D1 reward versus D2 ambivalence. *PLoS One*, 13, e0207694. <https://doi.org/10.1371/journal.pone.0207694>
- Dalley, J. W., Lääne, K., Theobald, D. E. H., Armstrong, H. C., Corlett, P. R., Chudasama, Y., & Robbins, T. W. (2005). Time-limited modulation of appetitive Pavlovian memory by D1 and NMDA receptors in the nucleus accumbens. *Proceedings of the National Academy of Sciences of the United States of America*, 102, 6189–6194. <https://doi.org/10.1073/pnas.0502080102>
- Day, J. J., & Carelli, R. M. (2007). The nucleus accumbens and Pavlovian reward learning. *The Neuroscientist*, 13, 148–159. <https://doi.org/10.1177/1073858406295854>

- Day, J. J., Jones, J. L., & Carelli, R. M. (2011). Nucleus accumbens neurons encode predicted and ongoing reward costs in rats. *The European Journal of Neuroscience*, 33, 308–321. <https://doi.org/10.1111/j.1460-9568.2010.07531.x>
- Day, J. J., Wheeler, R. A., Roitman, M. F., & Carelli, R. M. (2006). Nucleus accumbens neurons encode Pavlovian approach behaviors: Evidence from an autoshaping paradigm. *European Journal of Neuroscience*, 23, 1341–1351. <https://doi.org/10.1111/j.1460-9568.2006.04654.x>
- de Jong, J. W., Afjei, S. A., Pollak Dorocic, I., Peck, J. R., Liu, C., Kim, C. K., Tian, L., Deisseroth, K., & Lammel, S. (2019). A neural circuit mechanism for encoding aversive stimuli in the mesolimbic dopamine system. *Neuron*, 101, 133–151.e7. <https://doi.org/10.1016/j.neuron.2018.11.005>
- Di Ciano, P., Cardinal, R. N., Cowell, R. A., Little, S. J., & Everitt, B. J. (2001). Differential involvement of NMDA, AMPA/Kainate, and dopamine receptors in the nucleus accumbens core in the acquisition and performance of Pavlovian approach behavior. *The Journal of Neuroscience*, 21, 9471–9477. <https://doi.org/10.1523/JNEUROSCI.21-23-09471.2001>
- Gale, J., Shields, D., Ishizawa, Y., & Eskandar, E. (2014). Reward and reinforcement activity in the nucleus accumbens during learning. *Frontiers in Behavioral Neuroscience*, 8, 114.
- Gallo, E. F. (2019). Disentangling the diverse roles of dopamine D2 receptors in striatal function and behavior. *Neurochemistry International*, 125, 35–46. <https://doi.org/10.1016/j.neuint.2019.01.022>
- Gerfen, C. R. (1984). The neostriatal mosaic: Compartmentalization of corticostriatal input and striatonigral output systems. *Nature*, 311, 461–464. <https://doi.org/10.1038/311461a0>
- Gerfen, C. R., Engber, T. M., Mahan, L. C., Susel, Z., Chase, T. N., Monsma, F. J., & Sibley, D. R. (1990). D1 and D2 dopamine receptor-regulated gene expression of striatonigral and striatopallidal neurons. *Science*, 250, 1429–1432. <https://doi.org/10.1126/science.2147780>
- Hikida, T., Kimura, K., Wada, N., Funabiki, K., & Nakanishi, S. (2010). Distinct roles of synaptic transmission in direct and indirect striatal pathways to reward and aversive behavior. *Neuron*, 66, 896–907. <https://doi.org/10.1016/j.neuron.2010.05.011>
- Hikida, T., Morita, M., & Macpherson, T. (2016). Neural mechanisms of the nucleus accumbens circuit in reward and aversive learning. *Neuroscience Research*, 108, 1–5. <https://doi.org/10.1016/j.neures.2016.01.004>
- Janak, P. H., Chen, M.-T., & Caulder, T. (2004). Dynamics of neural coding in the accumbens during extinction and reinstatement of rewarded behavior. *Behavioural Brain Research*, 154, 125–135. <https://doi.org/10.1016/j.bbr.2004.02.003>
- Jean-Richard-dit-Bressel, P., Clifford, C. W. G., & McNally, G. P. (2020). Analyzing event-related transients: Confidence intervals, permutation tests, and consecutive thresholds. *Frontiers in Molecular Neuroscience*, 13, 14. <https://doi.org/10.3389/fnmol.2020.00014>
- Kravitz, A. V., Tye, L. D., & Kreitzer, A. C. (2012). Distinct roles for direct and indirect pathway striatal neurons in reinforcement. *Nature Neuroscience*, 15, 816–818. <https://doi.org/10.1038/nn.3100>
- Kupchik, Y. M., Brown, R. M., Heinsbroek, J. A., Lobo, M. K., Schwartz, D. J., & Kalivas, P. W. (2015). Coding the direct/indirect pathways by D1 and D2 receptors is not valid for accumbens projections. *Nature Neuroscience*, 18, 1230–1232. <https://doi.org/10.1038/nn.4068>
- Le Moine, C., Normand, E., & Bloch, B. (1991). Phenotypical characterization of the rat striatal neurons expressing the D1 dopamine receptor gene. *Proceedings of the National Academy of Sciences of the United States of America*, 88, 4205–4209. <https://doi.org/10.1073/pnas.88.10.4205>
- Lee, R. S., Mattar, M. G., Parker, N. F., Witten, I. B., & Daw, N. D. (2019). Reward prediction error does not explain movement selectivity in DMS-projecting dopamine neurons. *eLife*, 8, e42992. <https://doi.org/10.7554/eLife.42992>
- Lobo, M. K., Covington, H. E., Chaudhury, D., Friedman, A. K., Sun, H., Damez-Werno, D., Dietz, D. M., Zaman, S., Koo, J. W., Kennedy, P. J., Mouzon, E., Mogri, M., Neve, R. L., Deisseroth, K., Han, M.-H., & Nestler, E. J. (2010). Cell type-specific loss of BDNF signaling mimics optogenetic control of cocaine reward. *Science*, 330, 385–390. <https://doi.org/10.1126/science.1188472>
- Namvar, P., Zarrabian, S., Nazari-Serenjeh, F., Sadeghzadeh, F., & Haghparast, A. (2019). Involvement of D1- and D2-like dopamine receptors within the rat nucleus accumbens in the maintenance of morphine rewarding properties in the rats. *Behavioral Neuroscience*, 133, 556–562. <https://doi.org/10.1037/bne0000336>
- Natsubori, A., Tsutsui-Kimura, I., Nishida, H., Boucheikiou, Y., Sekiya, H., Uchigashima, M., Watanabe, M., de Kerchove, d'E. A., Mimura, M., Takata, N., & Tanaka, K. F. (2017). Ventrolateral striatal medium spiny neurons positively regulate food-incentive, goal-directed behavior independently of D1 and D2 selectivity. *The Journal of Neuroscience*, 37, 2723–2733. <https://doi.org/10.1523/JNEUROSCI.3377-16.2017>
- Parker, N. F., Cameron, C. M., Taliaferro, J. P., Lee, J., Choi, J. Y., Davidson, T. J., Daw, N. D., & Witten, I. B. (2016). Reward and choice encoding in terminals of midbrain dopamine neurons depends on striatal target. *Nature Neuroscience*, 19, 845–854. <https://doi.org/10.1038/nn.4287>
- Parkinson, J. A., Dalley, J. W., Cardinal, R. N., Bamford, A., Fehner, B., Lachenal, G., Rudarakanchana, N., Halkerston, K. M., Robbins, T. W., & Everitt, B. J. (2002). Nucleus accumbens dopamine depletion impairs both acquisition and performance of appetitive Pavlovian approach behaviour: Implications for mesoaccumbens dopamine function. *Behavioural Brain Research*, 137, 149–163. [https://doi.org/10.1016/S0166-4328\(02\)00291-7](https://doi.org/10.1016/S0166-4328(02)00291-7)
- Patriarchi, T., Cho, J. R., Merten, K., Howe, M. W., Marley, A., Xiong, W.-H., Folk, R. W., Broussard, G. J., Liang, R., Jang, M. J., Zhong, H., Dombek, D., von Zastrow, M., Nimmerjahn, A., Gradinaru, V., Williams, J. T., & Tian, L. (2018). Ultrafast neuronal imaging of dopamine dynamics with designed genetically encoded sensors. *Science*, 360, eaat4422. <https://doi.org/10.1126/science.aat4422>
- Pavlov, I. P. (2010). Conditioned reflexes: An investigation of the physiological activity of the cerebral cortex. *Annals of Neurosciences*, 17, 136–141. <https://doi.org/10.5214/ans.0972-7531.1017309>
- Paxinos, G., & Franklin, K. B. J. (2001). *The mouse brain in stereotaxic coordinates* (2nd ed.). Academic Press.
- Ray, M. H., Moaddab, M., & McDannald, M. A. (2022). Threat and bidirectional valence signaling in the nucleus accumbens core. *The Journal of Neuroscience*, 42, 817–833. <https://doi.org/10.1523/JNEUROSCI.1107-21.2021>
- Rescorla, R. A. (1994). Control of instrumental performance by Pavlovian and instrumental stimuli. *Journal of Experimental Psychology: Animal Behavior Processes*, 20, 44–50. <https://doi.org/10.1037/0097-7403.20.1.44>
- Roitman, M. F., Wheeler, R. A., & Carelli, R. M. (2005). Nucleus accumbens neurons are innately tuned for rewarding and aversive taste stimuli, encode their predictors, and are linked to motor output. *Neuron*, 45, 587–597. <https://doi.org/10.1016/j.neuron.2004.12.055>
- Setlow, B., Schoenbaum, G., & Gallagher, M. (2003). Neural encoding in ventral striatum during olfactory discrimination learning. *Neuron*, 38, 625–636. [https://doi.org/10.1016/S0896-6273\(03\)00264-2](https://doi.org/10.1016/S0896-6273(03)00264-2)
- Sherathiya, V. N., Schaid, M. D., Seiler, J. L., Lopez, G. C., & Lerner, T. N. (2021). GuPPy, a python toolbox for the analysis of fiber photometry data. *Scientific Reports*, 11, 24212. <https://doi.org/10.1038/s41598-021-03626-9>
- Skirzewski, M., Princz-Lebel, O., German-Castelan, L., Crooks, A. M., Kim, G. K., Tarnow, S. H., Reichelt, A., Memar, S., Palmer, D., Li, Y., Jane Rylett, R., Saksida, L. M., Prado, V. F., Prado, M. A. M., & Bussey, T. J. (2022). Continuous cholinergic-dopaminergic updating in the nucleus accumbens underlies approaches to reward-predicting cues. *Nature Communications*, 13, 7924. <https://doi.org/10.1038/s41467-022-35601-x>



- Soares-Cunha, C., Coimbra, B., David-Pereira, A., Borges, S., Pinto, L., Costa, P., Sousa, N., & Rodrigues, A. J. (2016). Activation of D2 dopamine receptor-expressing neurons in the nucleus accumbens increases motivation. *Nature Communications*, 7, 11829. <https://doi.org/10.1038/ncomms11829>
- Soares-Cunha, C., Coimbra, B., Domingues, A. V., Vasconcelos, N., Sousa, N., & Rodrigues, A. J. (2018). Nucleus accumbens microcircuit underlying D2-MSN-driven increase in motivation. *eNeuro*, 5, ENEURO.0386-18.2018. <https://doi.org/10.1523/ENEURO.0386-18.2018>
- Soares-Cunha, C., de Vasconcelos, N. A. P., Coimbra, B., Domingues, A. V., Silva, J. M., Loureiro-Campos, E., Gaspar, R., Sotiropoulos, I., Sousa, N., & Rodrigues, A. J. (2020). Nucleus accumbens medium spiny neurons subtypes signal both reward and aversion. *Molecular Psychiatry*, 25, 3241-3255. <https://doi.org/10.1038/s41380-019-0484-3>
- Soares-Cunha, C., Domingues, A. V., Correia, R., Coimbra, B., Vieitas-Gaspar, N., de Vasconcelos, N. A. P., Pinto, L., Sousa, N., & Rodrigues, A. J. (2022). Distinct role of nucleus accumbens D2-MSN projections to ventral pallidum in different phases of motivated behavior. *Cell Reports*, 38, 110380. <https://doi.org/10.1016/j.celrep.2022.110380>
- Soares-Cunha, C., & Heinsbroek, J. A. (2023). Ventral pallidal regulation of motivated behaviors and reinforcement. *Frontiers in Neural Circuits*, 17, 1086053. <https://doi.org/10.3389/fncir.2023.1086053>
- Volman, S. F., Lammel, S., Margolis, E. B., Kim, Y., Richard, J. M., Roitman, M. F., & Lobo, M. K. (2013). New insights into the specificity and plasticity of reward and aversion encoding in the mesolimbic

system. *The Journal of Neuroscience*, 33, 17569-17576. <https://doi.org/10.1523/JNEUROSCI.3250-13.2013>

- Wan, X., & Peoples, L. L. (2006). Firing patterns of accumbal neurons during a Pavlovian-conditioned approach task. *Journal of Neurophysiology*, 96, 652-660. <https://doi.org/10.1152/jn.00068.2006>
- Yanagimoto, K., & Maeda, H. (2003). The nucleus accumbens unit activities related to the emotional significance of complex environmental stimuli in freely moving cats. *Neuroscience Research*, 46, 183-189. [https://doi.org/10.1016/s0168-0102\(03\)00058-0](https://doi.org/10.1016/s0168-0102(03)00058-0)

SUPPORTING INFORMATION

Additional supporting information can be found online in the Supporting Information section at the end of this article.

How to cite this article: Deseyve, C., Domingues, A. V., Carvalho, T. T. A., Armada, G., Correia, R., Vieitas-Gaspar, N., Wezik, M., Pinto, L., Sousa, N., Coimbra, B., Rodrigues, A. J., & Soares-Cunha, C. (2024). Nucleus accumbens neurons dynamically respond to appetitive and aversive associative learning. *Journal of Neurochemistry*, 00, 1-16. <https://doi.org/10.1111/jnc.16063>